AEM Journals.ASM.org

Breaking the Silence: Protein Stabilization Uncovers Silenced Biosynthetic Gene Clusters in the Fungus *Aspergillus nidulans*

Jennifer Gerke,[a] Özgür Bayram,[a] Kirstin Feussner,[a,b] Manuel Landesfeind,[c] Ekaterina Shelest,[d] Ivo Feussner,[b] and Gerhard H. Braus[a]

Abteilung für Molekulare Mikrobiologie & Genetik, Institut für Mikrobiologie & Genetik, Georg August Universität, Göttingen, Germany[a]; Abteilung Biochemie der Pflanze, Albrecht von Haller Institut für Pflanzenwissenschaften, Georg August Universität, Göttingen, Germany[b]; Abteilung für Bioinformatik, Institut für Mikrobiologie & Genetik, Georg August Universität, Göttingen, Germany[c]; and Forschungsgruppe Systembiologie/Bioinformatik, Leibniz Institut für Naturstoff-Forschung und Infektionsbiologie, Hans Knöll Institut, Jena, Germany[d]

The genomes of filamentous fungi comprise numerous putative gene clusters coding for the biosynthesis of chemically and structurally diverse secondary metabolites (SMs), which are rarely expressed under laboratory conditions. Previous approaches to activate these genes were based primarily on artificially targeting the cellular protein synthesis apparatus. Here, we applied an alternative approach of genetically impairing the protein degradation apparatus of the model fungus *Aspergillus nidulans* by deleting the conserved eukaryotic *csnE/CSN5* deneddylase subunit of the COP9 signalosome. This defect in protein degradation results in the activation of a previously silenced gene cluster comprising a polyketide synthase gene producing the antibiotic 2,4-dihydroxy-3-methyl-6-(2-oxopropyl)benzaldehyde (DHMBA). The *csnE/CSN5* gene is highly conserved in fungi, and therefore, the deletion is a feasible approach for the identification of new SMs.

Since its discovery by Fleming in the 1920s, fungal penicillin has saved the lives of millions. Currently, the World Health Organization forecasts that the dramatic increase in antimicrobial resistance all over the world might lead to a disaster and proclaims a need for novel drugs (22). Certain fungi, plants, and bacteria produce various potent secondary metabolites (SMs) that span a wide field of structurally and chemically diverse natural products. With almost 1.5 million species (33), the fungal kingdom is a major reservoir for bioactive natural products as beneficial antibiotics and antitumor drugs but also as deleterious mycotoxins and food contaminants (28, 38). Although many fungal SMs have been described and tested, their complete potential is by far not exploited.

In recent years, different approaches were applied to find novel bioactive SMs either in new species or in already established model organisms. New geographical spots exhibiting extreme conditions were explored in order to find new species producing as-yet-unknown natural products (37). An alternative approach is the exploration of the full genomic potential of already known species by genomic mining (13, 14, 30, 76). Genomic sequencing revealed that there are many more genes for the biosynthesis of SMs than the metabolites already identified. These genes are often clustered, but most of them are rarely expressed under laboratory conditions (35), making the identification of their chemical products challenging. Two major strategies were applied to activate hidden genes: (i) changing the environment or (ii) genetic engineering (19, 35, 56). (i) The OSMAC (one strain, many compounds) approach activates silent gene clusters by cultivating microorganisms under different conditions (10, 75). Alternatively, physical contact with an opponent results in the uncovering of hidden clusters by activating defense mechanisms (58). (ii) Genetic engineering is focused primarily on expressing complete gene clusters in heterologous hosts (53, 77) or on altering the cellular transcription or protein synthesis machinery. Thus, SM synthesis was enhanced by changing genes with regulatory (12, 59), ribosomal (36, 49), protein-modifying (57, 64), or chromatin-modifying (11, 48, 61) functions or by adding epigenetic modifiers with DNA methyltransferase or histone deacetylase inhibiting function (26, 34, 70). A more selective approach is the artificial expression of a specific transcription factor (TF) gene embedded in a silenced gene cluster, which is able to activate SM synthesis (8, 20), or the direct expression of the biosynthetic genes by an inducible promoter (1).

Here, we describe the proof of principle of an alternative genetic approach to discover products of silent SM genes by impairing the control of the protein destruction machinery. Most nuclear and cytoplasmic proteins, including many TFs, are degraded by the proteasome pathway, which requires the ubiquitin labeling of target proteins. The activity of the multiprotein COP9 signalosome complex (CSN) plays a crucial role in controlling this process (71). In its fifth subunit, CSN5/CsnE, there resides a deneddylase catalytic activity, which detaches the ubiquitin-like protein Nedd8 from cullin-based ubiquitin E3 ligases. The covalent linkage of Nedd8 to a lysine residue of cullins activates E3 enzymes, which control ubiquitin-mediated protein degradation in the cell (15). The deletion of the gene for CSN5/CsnE, which is highly conserved in eukaryotes, results in embryonic death in plants or animals but results in viable fungal mutant strains altered in secondary metabolism and development (69). This suggests that regulators of secondary metabolism and development cannot be degraded properly, resulting in the false expression of SM genes. We used this approach in combination with a recently established technique targeting TFs (8, 20) to identify as-yet-undescribed SM clusters for the model ascomycete *Aspergillus nidulans*. Genomic sequencing predicted 32 polyketide synthases (PKSs), 27 nonribosomal peptide (NRP) synthases, and 6 dimethyl-allyl-tryptophan

Received 4 June 2012 **Accepted** 11 September 2012
Published ahead of print 21 September 2012
Address correspondence to Gerhard H. Braus, gbraus@gwdg.de.
Supplemental material for this article may be found at http://aem.asm.org/.

doi:10.1128/AEM.01808-12

synthetases in *A. nidulans* (12, 58, 66), but only a few of them have been identified. The control of secondary metabolism and development is coordinated at the molecular level (5, 6, 74) and requires an intact CSN (15, 17, 18). The identification and deletion of the conserved *CSN5/csnE* genes might be accomplished even if an interesting fungal genome is not yet sequenced. Therefore, fungal *CSN5/csnE* mutant strains are an interesting reservoir for the discovery of novel SMs.

MATERIALS AND METHODS

Strains and growth conditions. Strains used in this study are listed in Table S1 in the supplemental material. *Aspergillus nidulans* strains were grown on minimal medium (0.52 g/liter KCl, 0.52 g/liter $MgSO_4$, 1.52 g/liter KH_2PO_4, 0.1% trace element solution [pH 6.5]) (4) at 30°C or 37°C and supplemented appropriately with 1 μg/ml pyridoxine-HCl, 1 μg/ml uracil, 0.25 μg/ml uridine, 1 μg/ml 4-aminobenzoic acid, 1 μg/ml pyrithiamine (TaKaRa Bio Inc., Münsing, Germany), 120 μg/ml nourseothricin-dihydrogen sulfate (clonNAT; Werner BioAgents, Jena, Germany), 80 μg/ml phleomycin (Cayla-InvivoGen, Toulouse, France), and 5 mg/plate DHMBA. D-Glucose (1%) served as the carbon source, and 10 mM nitrate or ammonium served as the nitrogen source. For solid medium, 2% agar was added. For the induction of sexual development, cultures were grown in the dark under oxygen limitation conditions, and for the induction of asexual development, cultures were grown in light (21). *Escherichia coli* strains DH5α and MACH-1 (Invitrogen GmbH, Karlsruhe, Germany) were used for the preparation of plasmid DNA and were cultivated in LB medium (1% tryptone, 0.5% yeast extract, 1% NaCl) supplemented with 100 μg/ml ampicillin or 50 μg/ml kanamycin. Bacterial strains for bioactivity tests were propagated on LB medium. *Sordaria macrospora* cells were grown on BMM medium (2.5% maize meal, 0.8% biomalt [pH 6.5]) (25). *Verticillium longisporum* cells were propagated on SXM medium (0.2% sodium pectin, 0.4% casein, 0.52 g/liter KCl, 0.52 g/liter $MgSO_4$, 1.52 g/liter KH_2PO_4, 0.1% trace element solution [pH 6.5]), and *Neurospora crassa* cultures were grown on Vogel's minimal medium with 2% sucrose (65). For MIC tests, *Micrococcus luteus* cells were grown in Mueller-Hinton broth (Carl Roth, Karlsruhe, Germany).

Strain and plasmid constructions. Strains and plasmids generated and used in this study are listed in Tables S1 and S2 in the supplemental material. For construction details, see the supplemental material.

Transformation procedures. Transformation in *A. nidulans* was performed by the polyethylene glycol-mediated fusion of protoplasts, as described previously (24). Transformation in *E. coli* was performed with calcium/manganese-treated cells (32).

Analysis of secondary metabolites. (i) General experimental procedures. ^{1}H nuclear magnetic resonance (NMR) spectra were recorded on Varian Mercury-Vx 300 (300 MHz) and Varian VNMRS-300 (300 MHz) spectrometers. ^{13}C-NMR spectra were recorded on a Varian Inova-500 spectrometer (125.7 MHz). Electrospray ionization mass spectrometry (ESI-MS) data were acquired by using a Finnigan LC-Q mass spectrometer. High-performance liquid chromatography (HPLC) was performed by using a system from Instrumentelle Analytik Goebel GmbH (for analytical HPLC, HPLC pump 420, SA 360 autosampler, Celeno UV-DAD HPLC detector, ELSD-Sedex 85 evaporative light-scattering detector (ERC), Nucleodur 250-mm by 3-mm 100-5 C_{18} end-capped (ec) column, and a solvent system where solvent A was H_2O plus 0.1% trifluoroacetic acid [TFA] and solvent B was acetonitrile plus 0.1% TFA; for preparative HPLC, Rainin Dynamax SD-1 HPLC pump, Rainin Dynamyx UV-1 HPLC detector, Nucleodur 250-mm by 20-mm 100-5 C_{18} ec column, and a solvent system where solvent A was H_2O and solvent B was acetonitrile).

(ii) Cultivation. One liter of liquid minimal medium with nitrate or ammonium as the nitrogen source was inoculated with 10^9 spores, and the culture was grown at 37°C for 36 h. For metabolic fingerprinting by ultra-performance liquid chromatography coupled with a time-of-flight mass spectrometer (UPLC–TOF-MS) (see Fig. 4D), cultures were grown for 10 days at 37°C in P flasks.

(iii) Extraction. Mycelia of cultures were removed by filtering with Miracloth, and the pH of the culture filtrate was adjusted to 5. The culture filtrate was extracted twice with an equivalent amount of ethyl acetate. The combined extracts were dried to yield the crude extract.

(iv) Analysis by HPLC coupled with a UV diode array detector (UV-DAD). The crude extracts were dissolved in 2 ml methanol (MeOH) and analyzed by HPLC using an analytical column under gradient conditions (20% solvent B to 100% solvent B in 20 min).

(v) Isolation of DHMBA. After ethyl acetate extraction, the crude extract of 2-liter cultures of strain AGB527 (grown in inducing medium) was extracted with CH_2Cl_2. The resulting extract was concentrated and chromatographed by preparative HPLC under gradient conditions (20% solvent B to 100% solvent B in 20 min, at a flow rate of 14 ml/min). Detection was carried out at 230 nm. DHMBA (3.9 mg) was eluted at 14.4 min. For detailed chemical data, see the supplemental material.

(vi) Isolation of DHPDI. The crude extract of 7-liter cultures of strain TNO (grown in inducing medium) was extracted with CH_2Cl_2. The resulting extract was concentrated and fractionated by preparative HPLC under gradient conditions (20% solvent B to 100% solvent B in 20 min, at a flow rate of 14 ml/min). Detection was carried out at 230 nm. The fraction which eluted at 12.0 min was further chromatographed on a Sephadex column by using MeOH as the solvent and yielded 1.4 mg of the compound 3,3-(2,3-dihydroxypropyl)diindole (DHPDI). For detailed chemical data, see the supplemental material.

Bioactivity tests. The potential antibiotic or antifungal activities of the isolated metabolites DHMBA and DHPDI were tested by agar diffusion tests. Twenty-five microliters of a methanolic solution of the substances ($c = 1$ mg/ml) was added onto sterile filter discs (diameter, 9 mm) and put onto agar plates inoculated with *Escherichia coli*, *Bacillus subtilis*, *Micrococcus luteus*, *Staphylococcus aureus*, *Salmonella enterica* serovar Typhimurium, *Agrobacterium tumefaciens*, *Pseudomonas fluorescens*, *Streptomyces griseus*, *Aspergillus fumigatus*, *Aspergillus nidulans*, *Verticillium longisporum*, *Neurospora crassa*, and *Sordaria macrospora*. Inhibition zones were measured after 1 to 5 days at 37°C or 25°C, respectively.

The MIC was determined by a microplate assay (44). *M. luteus* cells were grown overnight in Mueller-Hinton broth, and the optical density (OD) was adjusted to 0.1. Twofold dilutions of DHMBA (2 mg/ml) and the reference antibiotic vancomycin (2 mg/ml) were prepared with the microtiter plates. Finally, the wells contained 100 μl of Mueller-Hinton broth with or without an inhibitor as a control. Twenty-five microliters of the bacterial suspension was added, and the plates were cultivated for up to 24 h at 30°C. The OD was measured at 630 nm with a microplate reader (InfiniTe M2000 [Monochromator]; Tecan, Crailsheim, Germany). Mueller-Hinton broth was used as a blank incubated under the same conditions. The MIC was calculated from the highest antibiotic dilution showing complete inhibition. The tests were performed independently in triplicate.

Metabolic fingerprinting by UPLC–TOF-MS. Two biological replicates of each sample were analyzed three times by UPLC (Acquity UPLC system; Waters Corporation) coupled with a photodiode array (PDA) detector (UPLC eLambda, 800 nm; Waters Corporation) and with an orthogonal time-of-flight mass spectrometer (LCT Premier; Waters Corporation) (see the supplemental material for detailed information).

Identification of a putative binding site for DbaA. For motif predictions, the intergenic regions of the genes *dbaA*, *dbaB*/*dbaC*, *dbaD*/*dbaE*, *dbaF*/*dbaG*, and *dbaH*/*dbaI* were submitted to the MEME tool (2). Only one motif was found for all five sequences with a *P* value of 10^{-6} to 10^{-7} (see Table S3 in the supplemental material). This motif was next submitted to the TOMTOM tool (31) for the identification of similarities to known TF binding sites. The motif showed significant similarities to the yeast $Zn(II)_2$-Cys_6 TFs RGT1 ($P = 10^{-3}$) and ECM22 ($P = 10^{-2}$). To check the specificity of the motif found for the cluster sequences, the FIMO tool (29) was run on the set of 25 sequences (5 cluster promoters plus 10 promoters up- and downstream of the cluster) (see Table S4 in the supplemental material). With a *P* value of 10^{-6}, all cluster-specific sites

A)

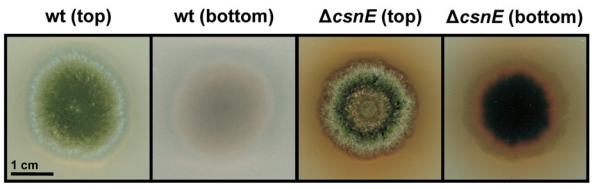

B)

Gene	log$_2$ contrast wt - Δ*csnE*				Regulation			
	V14	V20	A48	S48	V14	V20	A48	S48
AN7893	-3.85	-6.70	-4.50	-4.25	↑	↑	↑	↑
AN7894	-3.10	-6.45	-4.10	-4.30	↗	↑	↑	↑
AN7895	-2.90	-4.95	-4.00	-4.40	↗	↑	↑	↑
dbaA	-3.35	-3.50	-3.05	-3.35	↑	↑	↗	↑
dbaB	-2.80	-5.90	-3.20	-3.40	↗	↑	↑	↑
dbaC	-3.25	-6.00	-3.50	-4.10	↑	↑	↑	↑
dbaD	-3.15	-4.05	-2.05	-1.25	↗	↑	↗	0
dbaE	-3.45	-6.00	-1.65	-2.10	↑	↑	0	↗
dbaF	-5.35	-3.85	-1.65	-2.95	↑	↑	0	↗
dbaG	-3.00	-2.40	-1.30	-1.15	↗	↗	0	0
dbaH	-3.50	-7.00	-4.10	-4.50	↑	↑	↑	↑
dbaI	-2.84	-1.64	-0.07	-0.76	↗	0	0	0

C)

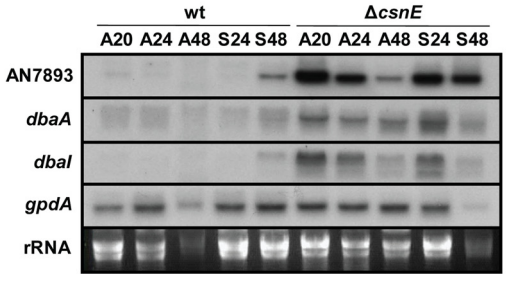

FIG 1 Deletion of the *csnE* subunit activates a novel putative biosynthetic gene cluster normally silenced in the wild type. (A) Phenotype of the wild-type (wt) and Δ*csnE* strains after 3 days of asexual growth at 37°C. Pictures were taken from the top and the bottom of agar plates. The Δ*csnE* mutant accumulates pigments around colony margins. (B) Transcriptional expression of genes in the Δ*csnE* mutant compared to the wild type at different developmental stages (V, vegetative; A, asexual; S, sexual; 14, 14 h; 20, 20 h; 48, 48 h). Genes with log$_2$ ratios of ≥3.2 and adjusted *P* values of ≤0.01 were regarded as being significantly regulated, and genes with log$_2$ ratios of ≥2 and adjusted *P* values of ≤0.01 were regarded as being moderately regulated. ↑, significantly upregulated; ↗, moderately upregulated; ↘, moderately downregulated; 0, not regulated. (C) Northern hybridization of three genes of the putative gene cluster. Samples were taken after 20, 24, and 48 h of asexual growth (A20, A24, and A48, respectively) and after 24 and 48 h of sexual growth (S24 and S48, respectively). Expression levels of *gpdA* and rRNA were used as internal controls. The expression levels of AN7893, *dbaA*, and *dbaI* were upregulated in the Δ*csnE* mutant compared to the wild type.

were recovered, whereas only one additional site (in the intergenic region between AN7893 and AN7894) was detected in the flanking promoters.

RESULTS

The *A. nidulans* Δ*csnE* mutant activates a silent biosynthetic gene cluster comprising a PKS gene. The *A. nidulans* Δ*csnE* mutant is deficient in the enzyme activity of COP9, which is involved in protein turnover control (45). The mutant is sensitive to oxidative stress (45) and accumulates pigments, which are absent in the wild type (Fig. 1A). Recently, we identified several of the pigments as orcinol and related phenylethers (45). Some of them were also found during an analysis of the recently identified orsellinic acid gene cluster comprising *orsA* to *orsE* (AN7909 to AN7914, respectively) (54).

We analyzed the protein-degradation-impaired *A. nidulans* Δ*csnE* mutant for its secondary metabolism by a genome-wide transcriptional profiling of Δ*csnE* mutant cells during development (45). Besides genes involved in sterigmatocystin (ST) (45) and orsellinic acid biosynthesis (see Table S5 in the supplemental material), the analysis revealed that an uncharacterized putative cluster containing a nonreducing PKS gene was upregulated in the Δ*csnE* strain but silenced in the wild type (AN7893 to AN7903) (Fig. 1B). The direct PKS product was recently identified as 2,4-dihydroxy-3-methyl-6-(2-oxopropyl)benzaldehyde (DHMBA) (1). The cluster genes were upregulated in comparison to the wild type in at least one developmental stage. We designated the genes of the putative cluster *dbaA* to *dbaI* (derivative of benzaldehyde), referring to the identified PKS gene product. The putative cluster spans 12 genes in total (Table 1). The cluster contains two putative TF-encoding genes, *dbaA*, with a Zn(II)$_2$-Cys$_6$ domain, and *dbaG*, encoding a protein with significant similarities to other putative fungal TFs (*Aspergillus fumigatus* [NCBI accession number *XP_*746385, 41% identities]). The initial microarray data were confirmed by Northern analysis of 3 randomly selected genes (AN7893, *dbaA*, and *dbaI*) of the new putative PKS gene cluster (Fig. 1C), suggesting that CSN is involved in the repression of this gene cluster in wild-type *A. nidulans* cells.

Northern hybridization determines the borders of the *dba* gene cluster. Numerous gene clusters carry a specific transcriptional activator (TF) gene which is embedded within the cluster (8, 20). To determine the boundaries of the novel gene cluster and to discriminate the effect on secondary metabolism, we designed strains overexpressing the putative TF-encoding gene *dbaA* or *dbaG*, respectively, under the control of the inducible nitrate reductase gene promoter (see Fig. S1 in the supplemental material). The overexpression of *dbaG* led to no significant changes in phenotype, whereas the overexpression of *dbaA* caused a strong extracellular pigmentation and a reduced growth diameter of the colony (Fig. 2A). Interestingly, the pigmentation depends on pH and is reversible: in neutral and basic milieus, the culture filtrate was yellow, while at a pH of <3, it turned colorless (Fig. 2B).

We performed Northern hybridization experiments with the *dbaA*-overexpressing (OE) and *dbaG*-OE strains (Fig. 2C). All genes starting from AN7893 to AN7909 (*orsA*) were used as probes, where we compared the promoter-repressing and -inducing conditions for the corresponding TF. The *dbaG*-overexpress-

TABLE 1 Encoded proteins of the *dba* gene cluster and their proposed functions[a]

Protein	Locus tag	Proposed function	Predicted length (aa)
DbaA	AN7896	Zn(II)$_2$-Cys$_6$ transcription factor	595
DbaB	AN7897	FAD-binding monooxygenase	393
DbaC	AN11584	Protein with YCII domain	109
DbaD	AN7898	General substrate transporter (MFS)	456
DbaE	AN7899	Esterase/lipase	278
DbaF	AN7900	FAD-dependent oxidoreductase	476
DbaG	AN7901	Putative fungal transcription factor (no conserved domain)	421
DbaH	AN7902	FAD binding monooxygenase	462
DbaI	AN7903	Nonreducing polyketide synthase	2,605

[a] aa, amino acids; FAD, flavin adenine dinucleotide.

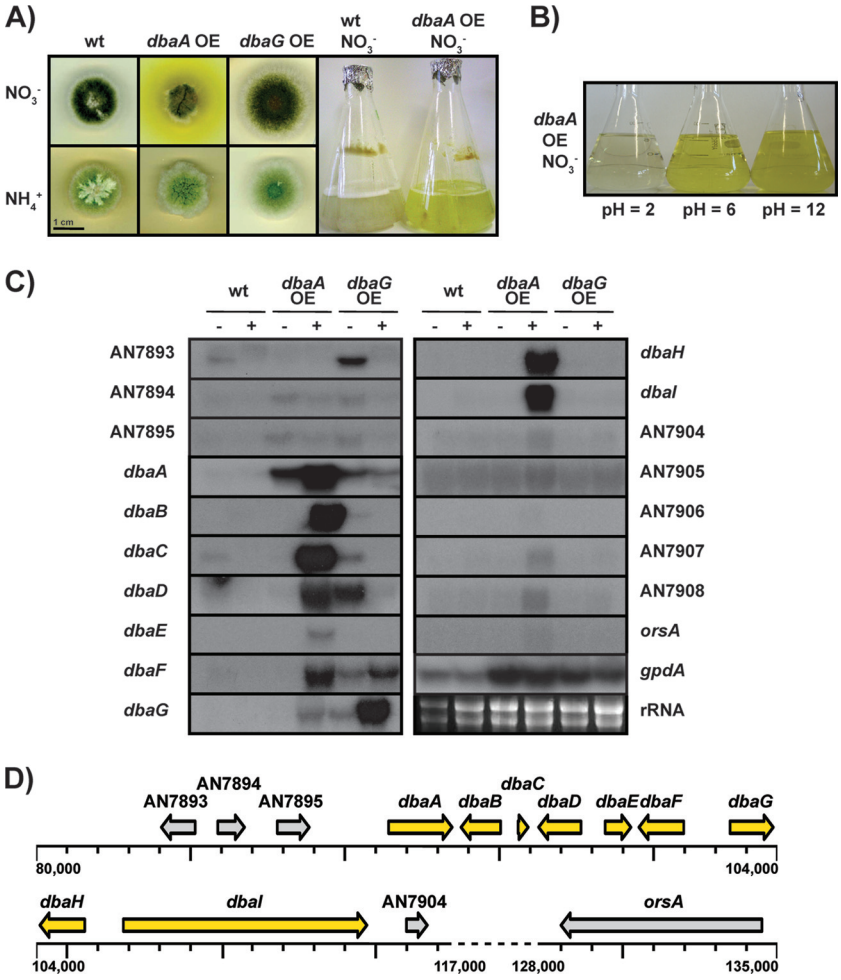

FIG 2 Boundaries of the *dba* gene cluster. (A) Phenotypes of *dbaA*- and *dbaG*-overexpressing strains. All strains were grown in inducing nitrate (NO_3^-) and repressing ammonium (NH_4^+) media. (B) Reversible pH dependency of yellow metabolites produced in the *dbaA*-OE strain grown in inducing nitrate medium for 24 h. (C) Northern hybridization of the genes AN7893 to *orsA* (AN7909) defines boundaries of the *dba* gene cluster. Strains were grown in inducing nitrate (+) and repressing ammonium (−) media. The expression level of *gpdA* was used as an internal control. The genes upregulated in both Northern and microarray analyses (Fig. 1B) were designated *dbaA* to *dbaI*. (D) Scheme of the *dba* gene cluster. The gene cluster contains the TF gene *dbaA* (AN7896); the oxygenase genes *dbaB* (AN7897), *dbaF* (AN7900), and *dbaH* (AN7902); the YCII domain gene *dbaC* (AN11584); the transporter gene *dbaD* (AN7898); the esterase/lipase gene *dbaE* (AN7899); the TF gene *dbaG* (AN7901); and the PKS gene *dbaI* (AN7903) (Table 1).

ing strain exhibited increased expression of the putative oxidoreductase gene *dbaF* only, whereas the expression levels of the AN7893, *dbaA*, *dbaC*, and *dbaD* genes even decreased.

In contrast, the overexpression of *dbaA* coordinately upregulated all consecutive genes from the AN7897 (*dbaB*) gene to the PKS-encoding AN7903 (*dbaI*) gene (Fig. 2C), indicating that these genes form a cluster which is controlled by the fungal $Zn(II)_2$-Cys_6 TF DbaA, encoded by the most 5′-upstream-located gene (AN7896) (Fig. 2D). DbaA also controls the second putative TF gene, *dbaG* (AN7901), suggesting a complex transcriptional control of the entire *dba* gene cluster.

By comparisons of the intergenic regions of the *dba* cluster (AN7896 and the intergenic regions between AN7897 and AN11584, AN7898 and AN7899, AN7900 and AN7901, and AN7902 and AN7903), a motif shared by all five sequences was found which is not present in the intergenic regions of the neighboring genes except for the intergenic region of AN7893/7894. A regulation for AN7893 (encoding a putative oxygenase) and AN7894 (encoding a putative YCII-related domain) was also detected in the transcriptome data (see Table S5 in the supplemental material) but not by Northern hybridization (Fig. 2C). The shared motif (CT/CCG/AGA/CG/CT/A/CA/TT/A/GC) shows significant similarities to the binding sites of the yeast $Zn(II)_2$-Cys_6 TFs RGT1 (Ykl038w) and ECM22 (YLR228C), corroborating our findings.

DHMBA and DHPDI are mutually exclusive metabolites. In order to identify the SMs produced by the *dba* gene cluster, wild-type and *dbaA*-OE strains were compared after cultivation in promoter-inducing medium. Culture filtrates were extracted with ethyl acetate and subsequently analyzed by high-performance liquid chromatography coupled with a UV diode array detector (HPLC–UV-DAD). The analysis revealed a major peak at the 10.3-min retention time with absorption maxima at 221 and 296 nm for the *dbaA*-OE strain and a peak at a 10.6-min retention time with absorption maxima at 231 and 276 nm for the wild-type strain (Fig. 3A). Interestingly, both peaks were mutually exclusive.

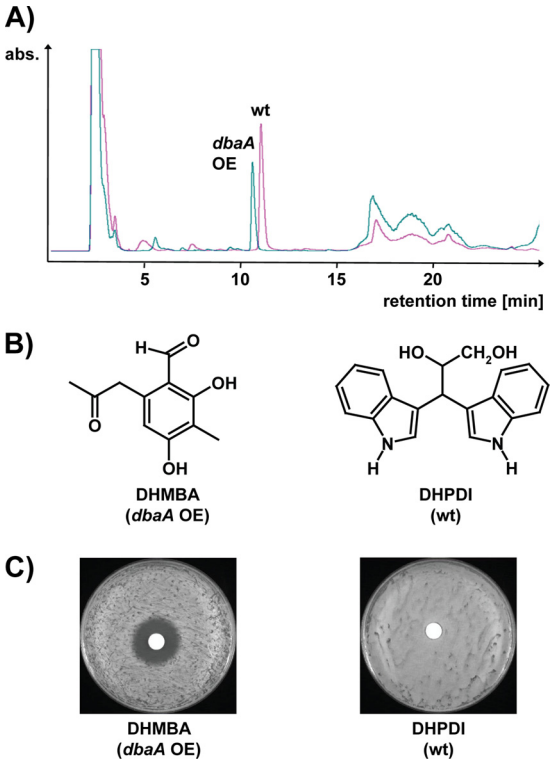

FIG 3 Identification of metabolites. (A) HPLC–UV-DAD chromatogram of the wild-type (magenta) and *dbaA*-OE (cyan) strains. abs., absorbance. (B) Chemical structures of 2,4-dihydroxy-3-methyl-6-(2-oxopropyl)benzaldehyde (DHMBA) and 3,3-(2,3-dihydroxypropyl)diindole (DHPDI). (C) Agar diffusion tests of DHMBA and DHPDI. Agar plates were inoculated with *Micrococcus luteus* cells and grown for 24 h at 37°C. Twenty-five microliters of DHMBA and DHPDI (1 mg/μl) was spotted onto filter discs. The inhibition zone of DHMBA was 2.5 cm.

We determined the structures of the two compounds by nuclear magnetic resonance (NMR) spectroscopy and mass spectrometry after cultivating both strains in larger amounts and applying different chromatographic methods for metabolite isolation (see Fig. S2A and S2B in the supplemental material).

The compound isolated from the *dbaA*-OE strain was identified as DHMBA (Fig. 3B), which was recently identified as a direct PKS product of DbaI (1). Interestingly, the UV spectrum of DHMBA was pH dependent. In the acidic milieu, the UV maxima were 221 and 296 nm, while with increasing pHs, the UV maxima shifted to higher values, 225, 295, and 340 nm in the neutral milieu and 257 and 341 nm in the basic milieu.

The compound isolated from the wild type was identified as the alkaloid 3,3-(2,3-dihydroxypropyl)diindole (DHPDI), which has not been described previously for aspergilli (Fig. 3B). Interestingly, the occurrence of DHPDI was medium dependent. After cultivation in nitrate medium, DHPDI was present, while in ammonium medium, the culture lacked DHPDI (see Fig. S2C in the supplemental material).

Besides the major peak, several minor peaks were present in the *dbaA*-overexpressing strain in the HPLC–UV-DAD chromatogram (retention times between 5 and 9 min) (Fig. 3A). Some of these peaks showed UV-visible (UV-Vis) maxima above 350 nm, indicating that these yellow components might contribute to the yellow color of the culture filtrate. Analysis by UPLC–TOF-MS revealed the exact masses of 21 compounds, which were produced in larger amounts in the *dbaA*-OE strain than in the wild type, 7 of which had UV maxima above 350 nm (see Table S6 in the supplemental material), indicating a yellow color.

DHMBA exhibits antibiotic activity in agar diffusion tests. We analyzed the putative antibiotic activities of DHMBA and DHPDI. In an initial screening, antibacterial and antifungal activities were tested by agar diffusion tests with different Gram-positive and Gram-negative bacteria as well as filamentous fungi (for a complete list, see Materials and Methods). The tests revealed no antibiotic activity for DHPDI. In contrast, DHMBA showed specific antibacterial activity against the Gram-positive bacterium *Micrococcus luteus*, with an inhibition zone of 2.5 cm in diameter after 24 h of growth (Fig. 3C). Thus, we determined the MIC of DHMBA against *M. luteus* in a microplate assay. The MIC was 3.1 μg/ml. This DHMBA-mediated antibacterial activity, which might contribute to the survival of the fungus, supports our approach of using *csnE* mutant strains for exploring the secondary metabolism potential for bioactive compounds of filamentous fungi.

Deletion of the PKS gene *dbaI* in the Δ*csnE* mutant results in the loss of numerous metabolite marker candidates, including DHMBA. For a comprehensive metabolite analysis of the *dba* gene cluster, we deleted the PKS-encoding gene *dbaI* in the wild-type and Δ*csnE* backgrounds (Fig. 4A; see also Fig. S3 in the supplemental material). The lack of *pks* transcripts was verified by Northern hybridization (Fig. 4B). As expected, due to the silencing of the cluster, the deletion of *dbaI* in the wild type caused no phenotypic changes, but in the Δ*csnE* mutant, the deletion resulted in an alteration of the Δ*csnE*-specific pigments surrounding the colony margin (Fig. 4A). The introduction of the *csnE* genomic fragment restored the wild-type and *dbaI* deletion phenotypes (not shown), and the ectopic introduction of the *dbaI* gene fused to the *gpdA* promoter restored the *csnE* deletion phenotype (Fig. 4A).

The metabolite production of the *A. nidulans* strain deficient in the COP9 signalosome was analyzed by a metabolite fingerprinting analysis. Extracellular ethyl acetate extracts of the wild-type, Δ*csnE*, Δ*dbaI*, and Δ*dbaI*/Δ*csnE* strains were analyzed by UPLC–TOF-MS. The intensity profiles of 895 marker candidates ($P < 1 \times 10^{-6}$) of the positive and negative ionization modes were clustered by training a one-dimensional self-organizing map (1D-SOM) model (42) and were grouped into 10 prototypes (Fig. 4C; see also Table S7 in the supplemental material). Prototypes 6 and 7 represent 184 marker candidates that were upregulated in the Δ*csnE* mutant but only when the PKS DbaI was present. Among them, DHMBA was detected in prototype 6 (Fig. 4D). Its production was enhanced in the Δ*csnE* mutant compared to wild-type levels but ceased when *dbaI* was deleted. Furthermore, the recently identified orsellinic acid (58) was detected in prototype 8 (Fig. 4D). As our microarray results suggested, its production was augmented in the Δ*csnE* mutant compared to the wild type. In the Δ*dbaI*/Δ*csnE* strain, orsellinic acid production was diminished but not ceased, indicating cross talk between the two PKSs DbaI and OrsA, as was suggested previously (46, 58).

Furthermore, we analyzed the influence of the TF DbaA on *dba* gene cluster expression in the Δ*csnE* mutant. Therefore, a *dbaA* deletion strain was constructed in the wild-type and Δ*csnE* backgrounds (see Fig. S3 in the supplemental material). Like the *pks* deletion, no phenotypic changes were observed in the wild-type

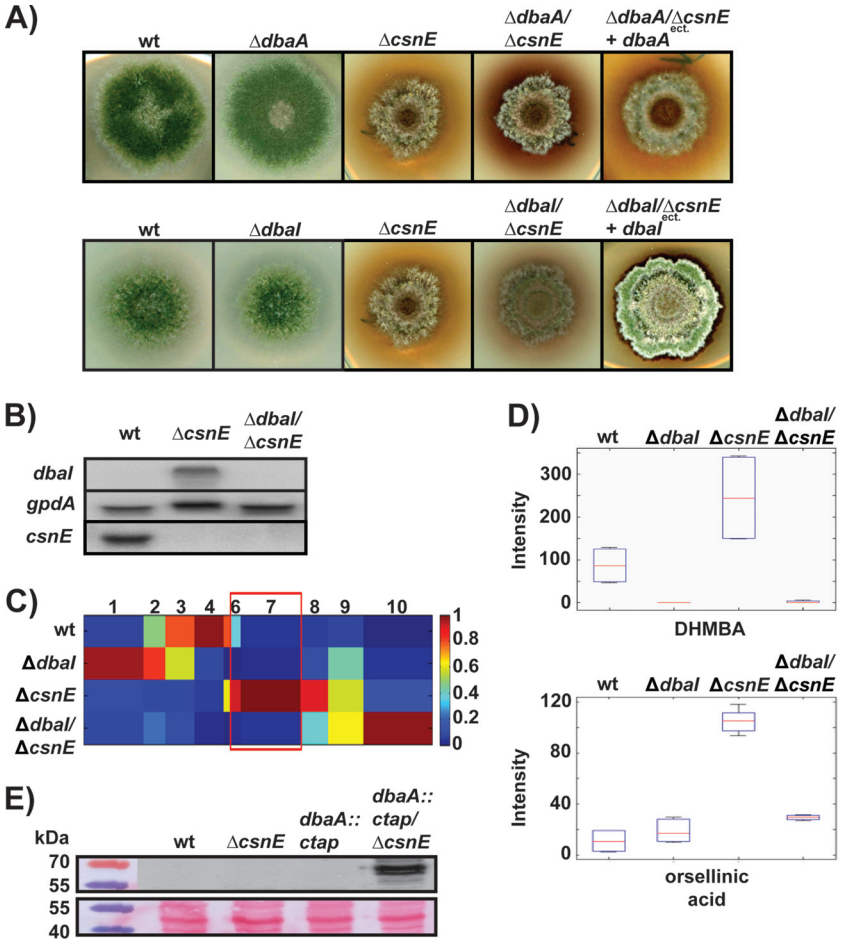

FIG 4 Metabolic fingerprinting of the Δ*csnE* and cluster mutants. (A) Phenotypes of TF *dbaA* and PKS *dbaI* gene deletions in wild-type and Δ*csnE* backgrounds. ect., ectopically integrated. (B) Northern hybridization of the Δ*dbaI*/Δ*csnE* deletion strain. Expression levels of *gpdA* and *csnE* were used as internal controls. (C) Clustering of the intensity profiles of 895 metabolite marker candidates of the ethyl acetate extraction phases of the wild-type, Δ*csnE*, Δ*dbaI*, and Δ*csnE*/Δ*dbaI* strains by 1D-SOM. The horizontal and vertical dimensions correspond to prototypes 1 to 10 and the analyzed fungus strains, respectively. Prototypes 6 and 7 (red frame) represent metabolite markers, which accumulate specifically in the Δ*csnE* strain. Colors of matrix elements represent average intensity values. For the complete data set, see Table S7 in the supplemental material. (D) Box-whisker plots showing the relative abundances of DHMBA, which was detected in prototype 6, and of orsellinic acid, which was detected in prototype 8. (E) Western blot of the C-terminally TAP-tagged TF DbaA. Ponceau staining is shown as an equal loading control.

background, while in the Δ*csnE* background, again, a change of pigments was observed (Fig. 4A). For the Δ*dbaA*/Δ*csnE* mutant, the deletion phenotype was restored by the ectopic integration of a *dbaA* genomic fragment.

We tested whether the deletion of *csnE* increases the amount of the TF DbaA. Therefore, we designed a *ctap* (tandem affinity purification [TAP])-tagged *dbaA* construct and expressed it in the wild-type and Δ*csnE* backgrounds (see Fig. S3 in the supplemental material). A Western blot experiment with the anti-calmodulin binding peptide antibody, recognizing the calmodulin binding peptide (CBP) of the TAP tag, showed strong production of DbaA in the Δ*csnE* background but not in the wild-type background (Fig. 4E). Our results suggest that protein levels of the TF DbaA accumulate in the absence of CsnE.

The oxygenase DbaH is required for yellow pigment production and is involved in sexual development. We designed deletion mutants of all *dba* genes in the *dbaA*-OE and wild-type backgrounds in order to deepen our understanding of the new gene cluster and its possible function (see Fig. S4 in the supplemental material). Phenotypes of all deletions are summarized in Fig. 5A. In the wild-type background, all deletions exhibited no obvious phenotype, presumably due to the silencing of the gene cluster. In the *dbaA*-OE background, the Δ*dbaB*, Δ*dbaC*, Δ*dbaE*, and Δ*dbaF* strains showed no phenotypic changes compared to the *dbaA*-OE strain. However, the Δ*dbaD*, Δ*dbaG*, and Δ*dbaH* strains largely lost the ability to produce yellow pigments. For the Δ*dbaD* and Δ*dbaG* strains, pigment production was observed only weakly in liquid but not on solid medium, and the Δ*dbaH* strain completely lost the yellow color and instead produced red pigments (see Fig. S5 in the supplemental material). Interestingly, all yellow strains had a reduced growth diameter, whereas the strains without yellow pigments had a growth diameter similar to that of the wild type (Fig. 5B), suggesting a toxic effect of secreted metabolites.

In addition, we analyzed the DHMBA production of the cluster deletion strains in the *dbaA*-OE background by HPLC analysis. All strains still produced DHMBA but in different amounts. While the Δ*dbaE*, Δ*dbaF*, and Δ*dbaG* strains pro-

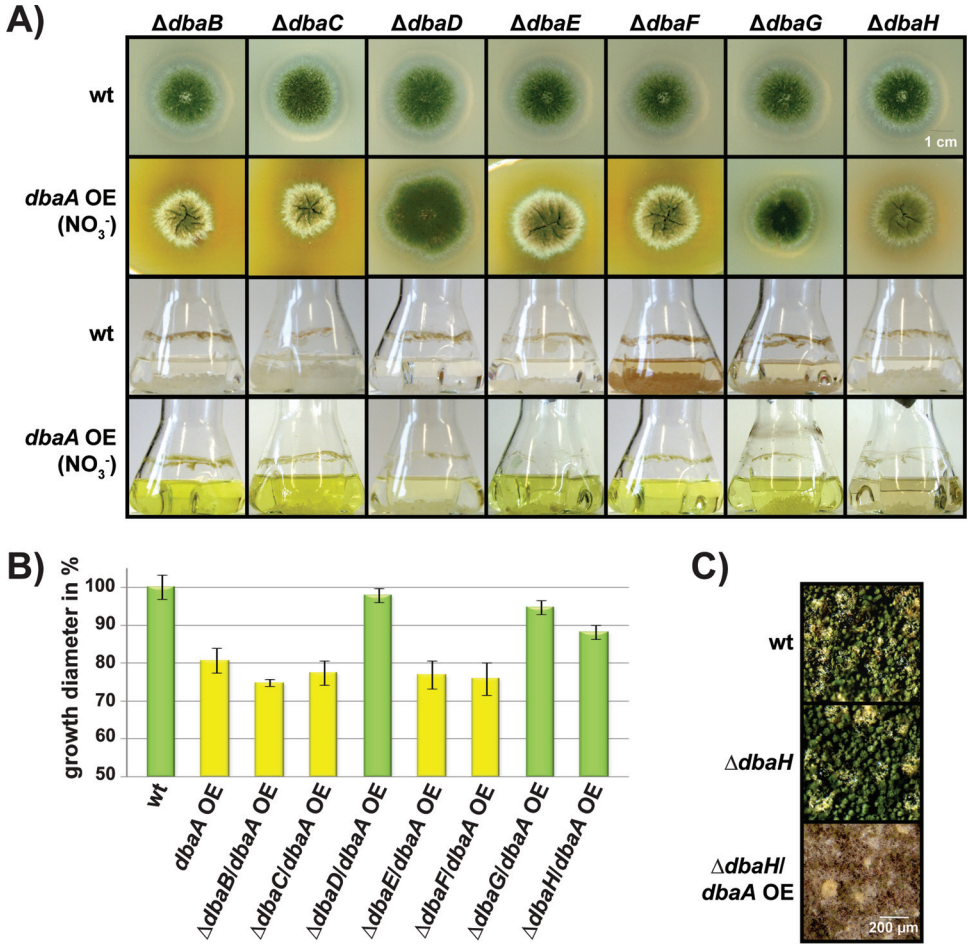

FIG 5 Phenotypes of *dba* cluster deletions in the wild-type and *dbaA*-OE backgrounds. (A) Growth test on inducing nitrate (NO_3^-) and repressing ammonium (NH_4^+) media. For asexual development, strains were grown for 3 days at 37°C in light. For the vegetative stage, strains were grown 24 h in liquid medium. (B) Growth diameters of cluster deletion colonies compared to the wild-type and *dbaA*-OE strains. The wild-type diameter was set to 100%. Strains were grown for 3 days in light on inducing nitrate medium. Green, no production of yellow metabolites; yellow, production of yellow metabolites. (C) Phenotypes for sexual development of the Δ*dbaH*/*dbaA*-OE, Δ*dbaH*, and wild-type strains. Strains were grown for 7 days at 37°C in the dark under conditions of limited oxygen levels. The Δ*dbaH*/*dbaA*-OE strain produces only a few cleistothecia with delayed pigmentation.

duced reduced DHMBA amounts, the production in the Δ*dbaH* strain was enriched (Fig. 6). As DbaD contains the major facilitator superfamily (MFS) transporter domain, we conclude that it might be involved in the transport of the metabolites to the environment. *dbaH* encodes a putative oxygenase, and due to the loss of yellow pigments and the accumulation of DHMBA in the deletion strain, we conclude that DbaH is responsible for the synthesis of yellow pigments derived from the oxidation of DHMBA. The block of this reaction by the deletion of *dbaH* led to the accumulation of the putative precursor DHMBA. In addition to metabolic changes, the developmental phenotype was altered in the Δ*dbaH*/*dbaA*-OE strain. The strain was impaired in sexual development and produced very few colorless but fertile sexual fruit bodies (cleistothecia) after 7 days of sexual growth (Fig. 5C). At this stage, cleistothecium formation in the wild-type strain was completed. The production of Hülle cells, which are nursing cells to support fruit body development (55), was not affected. The few cleistothecia gained color after 10 days of growth. However, the exogenous addition of purified DHMBA to the growth medium of the Δ*dbaH* strain resulted in no change in sexual development.

Our results suggest that the *dba* gene cluster has impacts not only on secondary metabolism but also on the developmental processes of the fungus.

DISCUSSION

The identification of silent and orphan gene clusters is of broad interest for biotechnology, including the pharmaceutical or food industry (9, 16, 27, 38). Only a fraction of all presumed biosynthetic genes and their products are known, and it is necessary to develop new tools for the activation of silent gene clusters. We showed here the successful application of a new approach to awaken silenced biosynthetic gene clusters. This approach is based on the idea that the interruption of the protein degradation machinery can lead to the increased stabilization of regulators, including transcriptional activators for biosynthetic gene clusters. We chose the deletion of the *csnE* gene, encoding a subunit of COP9 (CSN), where we had observed metabolic changes in previous studies (17, 45). The multiprotein complex CSN is highly conserved in eukaryotes (68) and plays a crucial role in the control of ubiquitin-mediated protein degradation in the cell (15). The *csnE* deletion mutant of *A. nidulans* is impaired in sexual repro-

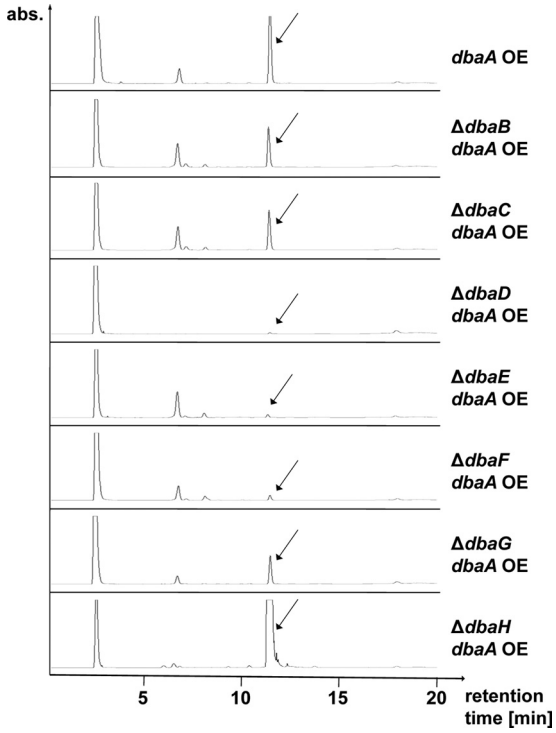

FIG 6 HPLC–UV-DAD chromatograms of cluster deletion strains in the *dbaA*-OE background. DHMBA is produced by all strains. In the Δ*dbaD*, Δ*dbaE*, and Δ*dbaF* strains, the level of DHMBA production was reduced, while in the Δ*dbaH* strain, production was enriched.

duction (15, 45) and produces the bioactive benzaldehyde DHMBA (Fig. 3B).

Previously established strategies to activate silent gene clusters can affect single or multiple pathways of an organism, depending on their respective targets. As all strategies have their advantages and disadvantages, it is necessary to select the appropriate approach for the respective issue. The environmental OSMAC approach or the "interspecies cross talk" approach can activate many different silenced gene clusters in an organism (10, 58, 75). However, it can be tedious and difficult to determine the specific growth conditions from a variety of parameters and organisms. The heterologous expression of a complete gene cluster in a different host organism attacks single pathways (53), but PKS- and NRPS-encoding gene clusters are especially very large, making this strategy challenging. The expression of TF-encoding genes located within a cluster by inducible promoters is another successful strategy (8, 20) but might require many gene clusters to be tested in a fungus. Unfortunately, gene clusters can also contain more than one or even lack TF-encoding genes. With our approach, we attacked the protein degradation machinery. In recent studies, only protein synthesis has been targeted by ribosome engineering (36, 49) or by targeting protein modifiers (57, 64). Our CSN5-based approach activates multiple biosynthetic gene clusters in an organism for the rapid identification of SMs. The advantages are that no deeper knowledge of possibly present gene clusters is necessary and that the amount of TFs in the cluster is primarily nonrelevant, although this method (8, 20) can be combined with our approach at a later stage of the analysis.

Transcriptional profiling of the *A. nidulans csnE* deletion strain showed previously that many designated secondary metabolism genes were misregulated (45). Besides the newly identified *dba* gene cluster controlled by the TF DbaA, the recently identified orsellinic acid gene cluster comprised of *orsA* to *orsE* (58) was also partially upregulated in the Δ*csnE* mutant (see Table S5 in the supplemental material), which was verified by 1D-SOM data showing orsellinic acid assigned to prototype 8 (Fig. 4D). Interestingly, the *dba* cluster is located directly 5′ upstream of the orsellinic acid gene cluster, and parts of the *dba* cluster were also upregulated during an orsellinic acid study reported previously by Nielsen et al. and Schroeckh et al. (46, 58). A cooperation of the PKSs DbaI and OrsA was hypothesized previously by Nielsen et al. (46). Those researchers showed that both PKS deletions led to a loss of F9775-A and F9775-B production, although both compounds could not be detected during our work.

The deduced amino acid sequences of the proteins encoded by the *dba* gene cluster (plus AN7893 to AN7895) were analyzed *in silico* in more detail. A BLAST (NCBI) search revealed that the amino acid sequences showed similarities to proteins of the citrinin-producing cluster of the mold *Monascus purpureus* and the methylorcinaldehyde-producing cluster of the mold *Acremonium strictum* (protein identities are given in Table S8 in the supplemental material). The structures of the tetraketide methylorcinaldehyde and DHMBA differ only in the ligand at the 3′ position of the phenol ring.

DHMBA was first isolated as a side product from the New Zealand fungus *Sepedonium chrysospermum* in 2006 (43) and was recently discovered in *Aspergillus nidulans* (1). Until 2006, it was known only as an intermediate in the chemical synthesis of azaphilones (63). Azaphilones are pigments with pyrone-quinone structures containing a highly oxygenated bicyclic core and quaternary center, like the yellow citrinin. Some of them show biological activities such as antimicrobial and antitumor activities (23, 50, 51, 73), and recently, the application of azaphilones as future food colorants was proposed (41). Several azaphilones have been identified from different fungal species, like *Monascus*, *Penicillium*, *Epicoccum*, and also *Aspergillus* species (20, 40, 60, 62), and recently, the first studies delivered insight into the biosynthetic pathway (20, 40). During the biosynthesis of asperfuranone, the first enzyme-free intermediate was identified as a benzaldehyde similar to DHMBA but differently substituted at the 6′ position (20). However, a hydroxylase-encoding gene is missing in the *dba* cluster to convert DHMBA to an azaphilone related to asperfuranone.

During feeding studies, 2,4-dihydroxy-3,5-dimethyl-6-(2-oxo-3-methylpropyl)benzaldehyde, a compound similar to DHMBA with two additional methyl groups, was identified as the first enzyme-free intermediate in the biosynthesis of citrinin (3). In accordance with this, we suggest that the PKS product DHMBA might also be an intermediate in the synthesis of an azaphilone related to citrinin. Osmanova et al. and Yang et al. even isolated metabolites from *Aspergillus* sp. synthesized from azaphilones and orsellinic acid (50, 72). Perhaps, the neighboring *dba* and *ors* clusters work together to synthesize metabolites related to those identified previously by Yang et al. (72), as both gene clusters are activated in the Δ*csnE* mutant.

The conversion of DHMBA to the yellow pigments found in the Δ*csnE* mutant or when *dbaA* is overexpressed might happen by the oxidation of DHMBA by the oxygenase DbaH, whose deletion results in the accumulation of DHMBA and a loss of yellow pig-

ments. Interestingly, the deletion of the oxygenase-encoding gene *dbaH* in the *dbaA*-OE background also led to impaired sexual development. The very few cleistothecia that were found were delayed in pigmentation. However, the exogenous addition of DHMBA to the growth medium of the Δ*dbaH* mutant had no influence on sexual behavior, showing that not the accumulated DHMBA but other pleiotropic effects might trigger the defects in sexual development. Nevertheless, we cannot exclude problems in the uptake of exogenous DHMBA of the cells. A correlation between PKS gene cluster expression and sexual development was recognized previously for *Neurospora crassa* and *Sordaria macrospora* (47). The deletion mutant of the oxygenase-encoding gene *fbm1*, which is member of a PKS gene cluster in both organisms, also showed the formation of fewer and delayed fruit bodies. Although the *dbaH* and *fbm1* sequences show no similarities, they might play a similar role in their organisms.

The follow-up experiments of our comparison of the *dbaA*-OE mutant and the wild type resulted in a second compound isolated from wild-type *A. nidulans*, which was 3,3-(2,3-dihydroxypropyl) diindole (DHPDI). This indole alkaloid was first found in mutants of *Saccharomyces cerevisiae*, which were blocked in tryptophan biosynthesis and accumulated different indole derivatives (39). Additionally, the toxic compound was isolated from the ergot-type symptom-causing fungus *Balansia epichloë* (52) and from the North Sea alphaproteobacterium *Oceanibulbus indolifex* (67), but to our knowledge, this is the first report of its isolation from aspergilli. Interestingly, the stability of DHPDI was pH dependent. While the diindole was stable in a basic milieu, at a pH of <3 it was converted into 2-oxo-3-indolyl-(3)-propan-1-ol, indole, and unknown indole polymers (39), which presumably explains the lack of DHPDI in ammonium-containing medium (see Fig. S2C in the supplemental material). After cultivation in ammonium medium, the pH of the cultures was around 2.4, while cultivation in nitrate medium resulted in a pH of 6.3.

Interestingly, the nitrogen-containing DHPDI, probably built up from tryptophan by a cryptic NRPS, is not produced anymore when *dbaA* is overexpressed. This might be due to pleiotropic effects but could also mean that there is an additional role of DbaA as a regulator for more than only one gene cluster. A recently reported study showed that TFs do not exclusively regulate the gene cluster in which they are embedded but that they are also able to navigate the cross talk between gene clusters located even on different chromosomes (7). Here, DbaA might additionally regulate the expression of the DHPDI-producing gene cluster. This could be a natural cross talk but also due to the misexpression of biosynthetic genes. Additionally, we identified the masses of 21 metabolites in the *dbaA*-OE strain, among them 3 nitrogen-containing compounds, which emphasizes our hypothesis of intercluster cross talk (see Table S6 in the supplemental material). In the Δ*csnE* strain, we observed a reduced level of production of the aflatoxin precursor sterigmatocystin (ST) (45), whereas the overexpression of *dbaA* did not affect ST production (Fig. S6), implying an independence of *dbaA* from the well-studied ST gene cluster.

Despite recent progress in the development of different strategies, the identification of silent SM-producing gene clusters still remains challenging. Our new approach based on interrupting the protein degradation system gives a new possibility to uncover hidden SMs in a broader manner. We showed for the model *A. nidulans*, as a paradigm of an SM-producing filamentous fungus, that the deletion of *CSN5/csnE* results in the activation of several clusters. We detected the PKS products DHMBA and orsellinic acid in the mutant, and additionally, we identified the new metabolite DHPDI from the wild type, which was so far not known to be produced by aspergilli. It will be interesting in the future to see what other SMs can be identified by further *csn* mutants from other fungi or even lower plants like algae, which also promise to have a high potential for bioactive molecules, which are urgently required to combat multidrug-resistant microbes.

ACKNOWLEDGMENTS

We thank BioViotica Naturstoffe GmbH for providing equipment for the isolation and identification of secondary metabolites. We appreciate the experimental support of K. Nahlik in the initial phase of the project and of P. Meyer and A. Kaever. We thank M. Hoppert, S. Pöggeler, P. Neumann-Staubitz, S. Seiler, and R. Daniel for providing strains for bioactivity tests. We thank B. Joehnk for proofreading the manuscript.

This work has been funded by grants from the Deutsche Forschungsgemeinschaft (DFG), the Volkswagen-Stiftung, and the Fonds der Chemischen Industrie to G.H.B.

REFERENCES

1. **Ahuja M, et al.** 2012. Illuminating the diversity of aromatic polyketide synthases in *Aspergillus nidulans.* J. Am. Chem. Soc. **134**:8212–8221.
2. **Bailey TL, Elkan C.** 1994. Fitting a mixture model by expectation maximization to discover motifs in biopolymers. Proc. Int. Conf. Intell. Syst. Mol. Biol. **2**:28–36.
3. **Barber J, Carter RH, Garson MJ, Staunton J.** 1981. The biosynthesis of citrinin by *Penicillium citrinum.* J. Chem. Soc. Perkin Trans. 1 **1981**:2577–2583.
4. **Barratt RW, Johnson GB, Ogata WN.** 1965. Wild-type and mutant stocks of *Aspergillus nidulans.* Genetics **52**:233–246.
5. **Bayram O, et al.** 2012. The Aspergillus nidulans MAPK module AnSte11-Ste50-Ste7-Fus3 controls development and secondary metabolism. PLoS Genet. **8**:e1002816. doi:10.1371/journal.pgen.1002816.
6. **Bayram O, et al.** 2008. VelB/VeA/LaeA complex coordinates light signal with fungal development and secondary metabolism. Science **320**:1504–1506.
7. **Bergmann S, et al.** 2010. Activation of a silent fungal polyketide biosynthesis pathway through regulatory cross talk with a cryptic nonribosomal peptide synthetase gene cluster. Appl. Environ. Microbiol. **76**:8143–8149.
8. **Bergmann S, et al.** 2007. Genomics-driven discovery of PKS-NRPS hybrid metabolites from *Aspergillus nidulans.* Nat. Chem. Biol. **3**:213–217.
9. **Blanc PJ, et al.** 1995. Characterization of monascidin A from *Monascus* as citrinin. Int. J. Food Microbiol. **27**:201–213.
10. **Bode HB, Bethe B, Hofs R, Zeeck A.** 2002. Big effects from small changes: possible ways to explore nature's chemical diversity. Chembiochem **3**:619–627.
11. **Bok JW, et al.** 2009. Chromatin-level regulation of biosynthetic gene clusters. Nat. Chem. Biol. **5**:462–464.
12. **Bok JW, et al.** 2006. Genomic mining for *Aspergillus* natural products. Chem. Biol. **13**:31–37.
13. **Brakhage A, Schroeckh V.** 2011. Fungal secondary metabolites—strategies to activate silent gene clusters. Fungal Genet. Biol. **48**:15–22.
14. **Brakhage AA, et al.** 2008. Activation of fungal silent gene clusters: a new avenue to drug discovery. Prog. Drug Res. **66**:1, 3-12.
15. **Braus GH, Irniger S, Bayram O.** 2010. Fungal development and the COP9 signalosome. Curr. Opin. Microbiol. **13**:672–676.
16. **Brodhagen M, Keller NP.** 2006. Signalling pathways connecting mycotoxin production and sporulation. Mol. Plant Pathol. **7**:285–301.
17. **Busch S, Eckert SE, Krappmann S, Braus GH.** 2003. The COP9 signalosome is an essential regulator of development in the filamentous fungus *Aspergillus nidulans.* Mol. Microbiol. **49**:717–730.
18. **Busch S, et al.** 2007. An eight-subunit COP9 signalosome with an intact JAMM motif is required for fungal fruit body formation. Proc. Natl. Acad. Sci. U. S. A. **104**:8089–8094.
19. **Chiang YM, Chang SL, Oakley BR, Wang CC.** 2011. Recent advances in awakening silent biosynthetic gene clusters and linking orphan clusters to natural products in microorganisms. Curr. Opin. Chem. Biol. **15**:137–143.

20. **Chiang YM, et al.** 2009. A gene cluster containing two fungal polyketide synthases encodes the biosynthetic pathway for a polyketide, asperfuranone, in *Aspergillus nidulans.* J. Am. Chem. Soc. **131**:2965–2970.
21. **Clutterbuck AJ.** 1974. *Aspergillus nidulans*, p 447–510. *In* King RC (ed), Handbook of genetics. Plenum Press, New York, NY.
22. **Cooper MA, Shlaes D.** 2011. Fix the antibiotics pipeline. Nature **472**:32. doi:10.1038/472032a.
23. **Dong J, et al.** 2006. New nematicidal azaphilones from the aquatic fungus *Pseudohalonectria adversaria* YMF1.01019. FEMS Microbiol. Lett. **264**:65–69.
24. **Eckert SE, Kubler E, Hoffmann B, Braus GH.** 2000. The tryptophan synthase-encoding *trpB* gene of *Aspergillus nidulans* is regulated by the cross-pathway control system. Mol. Gen. Genet. **263**:867–876.
25. **Esser K.** 1982. Cryptogams: cyanobacteria, algae, fungi, lichens. Textbook and practical guide. Cambridge University Press, Cambridge, United Kingdom.
26. **Fisch KM, et al.** 2009. Chemical induction of silent biosynthetic pathway transcription in *Aspergillus niger.* J. Ind. Microbiol. **36**:1199–1213.
27. **Frisvad JC, et al.** 2007. Secondary metabolite profiling, growth profiles and other tools for species recognition and important *Aspergillus* mycotoxins. Stud. Mycol. **59**:31–37.
28. **Garcia-Estrada C, et al.** 2011. A single cluster of coregulated genes encodes the biosynthesis of the mycotoxins roquefortine C and meleagrin in *Penicillium chrysogenum.* Chem. Biol. **18**:1499–1512.
29. **Grant CE, Bailey TL, Noble WS.** 2011. FIMO: scanning for occurrences of a given motif. Bioinformatics **27**:1017–1018.
30. **Gross H.** 2009. Genomic mining—a concept for the discovery of new bioactive natural products. Curr. Opin. Drug Discov. Devel. **12**:207–219.
31. **Gupta S, Stamatoyannopoulos JA, Bailey TL, Noble WS.** 2007. Quantifying similarity between motifs. Genome Biol. **8**:R24. doi:10.1186/gb-2007-8-2-r24.
32. **Hanahan D, Jessee J, Bloom FR.** 1991. Plasmid transformation of *Escherichia coli* and other bacteria. Methods Enzymol. **204**:63–113.
33. **Hawksworth DL, Rossman AY.** 1997. Where are all the undescribed fungi? Phytopathology **87**:888–891.
34. **Henrikson JC, Hoover AR, Joyner PM, Cichewicz RH.** 2009. A chemical epigenetics approach for engineering the in situ biosynthesis of a cryptic natural product from *Aspergillus niger.* Org. Biomol. Chem. **7**:435–438.
35. **Hertweck C.** 2009. Hidden biosynthetic treasures brought to light. Nat. Chem. Biol. **5**:450–452.
36. **Hosaka T, et al.** 2009. Antibacterial discovery in actinomycetes strains with mutations in RNA polymerase or ribosomal protein S12. Nat. Biotechnol. **27**:462–464.
37. **Keller M, Zengler K.** 2004. Tapping into microbial diversity. Nat. Rev. Microbiol. **2**:141–150.
38. **Keller NP, Turner G, Bennett JW.** 2005. Fungal secondary metabolism—from biochemistry to genomics. Nat. Rev. Microbiol. **3**:937–947.
39. **Lingens F, Göbel W.** 1967. Zur Biosynthese des Tryptophans in *Saccharomyces cerevisiae.* Biochim. Biophys. Acta **148**:70–83.
40. **Liu T, Chiang YM, Somoza AD, Oakley BR, Wang CC.** 2011. Engineering of an "unnatural" natural product by swapping polyketide synthase domains in *Aspergillus nidulans.* J. Am. Chem. Soc. **133**:13314–13316.
41. **Mapari SA, Thrane U, Meyer AS.** 2010. Fungal polyketide azaphilone pigments as future natural food colorants? Trends Biotechnol. **28**:300–307.
42. **Meinicke P, et al.** 2008. Metabolite-based clustering and visualization of mass spectrometry data using one-dimensional self-organizing maps. Algorithms Mol. Biol. **3**:9. doi:10.1186/1748-7188-3-9.
43. **Mitova MI, et al.** 2006. Chrysosporide, a cyclic pentapeptide from a New Zealand sample of the fungus *Sepedonium chrysospermum.* J. Nat. Prod. **69**:1481–1484.
44. **Mota-Meira M, LaPointe G, Lacroix C, Lavoie MC.** 2000. MICs of mutacin B-Ny266, nisin A, vancomycin, and oxacillin against bacterial pathogens. Antimicrob. Agents Chemother. **44**:24–29.
45. **Nahlik K, et al.** 2010. The COP9 signalosome mediates transcriptional and metabolic response to hormones, oxidative stress protection and cell wall rearrangement during fungal development. Mol. Microbiol. **78**:964–979.
46. **Nielsen ML, et al.** 2011. A genome-wide polyketide synthase deletion library uncovers novel genetic links to polyketides and meroterpenoids in *Aspergillus nidulans.* FEMS Microbiol. Lett. **321**:157–166.
47. **Nowrousian M.** 2009. A novel polyketide biosynthesis gene cluster is involved in fruiting body morphogenesis in the filamentous fungi *Sordaria macrospora* and *Neurospora crassa.* Curr. Genet. **55**:185–198.
48. **Nutzmann HW, et al.** 2011. Bacteria-induced natural product formation in the fungus *Aspergillus nidulans* requires Saga/Ada-mediated histone acetylation. Proc. Natl. Acad. Sci. U. S. A. **108**:14282–14287.
49. **Ochi K, et al.** 2004. Ribosome engineering and secondary metabolite production. Adv. Appl. Microbiol. **56**:155–184.
50. **Osmanova N, Schultze W, Ayoub N.** 2010. Azaphilones: a class of fungal metabolites with diverse biological activities. Phytochem. Rev. **9**:315–342.
51. **Phonkerd N, et al.** 2008. Bis-spiro-azaphilones and azaphilones from the fungi *Chaetomium cochliodes* VTh01 and *C. cochliodes* CTh05. Tetrahedron **64**:9636–9645.
52. **Porter JK, Bacon CW, Robbins JD, Himmelsbach DS, Higman HC.** 1977. Indole alkaloids from *Balansia epichloe* (Weese). J. Agric. Food Chem. **25**:88–93.
53. **Sakai K, Kinoshita H, Shimizu T, Nihira T.** 2008. Construction of a citrinin gene cluster expression system in heterologous *Aspergillus oryzae.* J. Biosci. Bioeng. **106**:466–472.
54. **Sanchez JF, et al.** 2010. Molecular genetic analysis of the orsellinic acid/F9775 gene cluster of *Aspergillus nidulans.* Mol. Biosyst. **6**:587–593.
55. **Sarikaya Bayram O, et al.** 2010. LaeA control of velvet family regulatory proteins for light-dependent development and fungal cell-type specificity. PLoS Genet. **6**:e1001226. doi:10.1371/journal.pgen.1001226.
56. **Scherlach K, Hertweck C.** 2009. Triggering cryptic natural product biosynthesis in microorganisms. Org. Biomol. Chem. **7**:1753–1760.
57. **Scherlach K, et al.** 2011. Cytotoxic pheofungins from an engineered fungus impaired in posttranslational protein modification. Angew. Chem. Int. Ed. Engl. **50**:9843–9847.
58. **Schroeckh V, et al.** 2009. Intimate bacterial-fungal interaction triggers biosynthesis of archetypal polyketides in *Aspergillus nidulans.* Proc. Natl. Acad. Sci. U. S. A. **106**:14558–14563.
59. **Shaaban MI, Bok JW, Lauer C, Keller NP.** 2010. Suppressor mutagenesis identifies a velvet complex remediator of *Aspergillus nidulans* secondary metabolism. Eukaryot. Cell **9**:1816–1824.
60. **Shao CL, et al.** 2011. Aspergilones A and B, two benzylazaphilones with an unprecedented carbon skeleton from the gorgonian-derived fungus *Aspergillus* sp. Bioorg. Med. Chem. Lett. **21**:690–693.
61. **Shwab EK, et al.** 2007. Histone deacetylase activity regulates chemical diversity in *Aspergillus.* Eukaryot. Cell **6**:1656–1664.
62. **Somoza AD, Lee KH, Chiang YM, Oakley BR, Wang CC.** 2012. Reengineering an azaphilone biosynthesis pathway in *Aspergillus nidulans* to create lipoxygenase inhibitors. Org. Lett. **14**:972–975.
63. **Suzuki T, et al.** 2001. Synthesis of 7-acetyloxy-3,7-dimethyl-7,8-dihydro-6H-isochromene-6,8-dione and its analogues. J. Heterocycl. Chem. **38**:1409–1418.
64. **Szewczyk E, et al.** 2008. Identification and characterization of the asperthecin gene cluster of *Aspergillus nidulans.* Appl. Environ. Microbiol. **74**:7607–7612.
65. **Vogel HJ.** 1956. A convenient growth medium for *Neurospora.* Microb. Genet. Bull. **13**:42–43.
66. **von Dohren H.** 2009. A survey of nonribosomal peptide synthetase (NRPS) genes in *Aspergillus nidulans.* Fungal Genet. Biol. **46**(Suppl 1):S45–S52. doi:10.1016/j.fgb.2008.08.008.
67. **Wagner-Dobler I, et al.** 2004. *Oceanibulbus indolifex* gen. nov., sp. nov., a North Sea alphaproteobacterium that produces bioactive metabolites. Int. J. Syst. Evol. Microbiol. **54**:1177–1184.
68. **Wei N, Chamovitz DA, Deng XW.** 1994. *Arabidopsis* COP9 is a component of a novel signaling complex mediating light control of development. Cell **78**:117–124.
69. **Wei N, Serino G, Deng XW.** 2008. The COP9 signalosome: more than a protease. Trends Biochem. Sci. **33**:592–600.
70. **Williams RB, Henrikson JC, Hoover AR, Lee AE, Cichewicz RH.** 2008. Epigenetic remodeling of the fungal secondary metabolome. Org. Biomol. Chem. **6**:1895–1897.
71. **Wu JT, Lin HC, Hu YC, Chien CT.** 2005. Neddylation and deneddylation regulate Cul1 and Cul3 protein accumulation. Nat. Cell Biol. **7**:1014–1020.
72. **Yang SW, et al.** 2009. Sch 1385568, a new azaphilone from *Aspergillus* sp. J. Antibiot. **62**:401–403.

73. **Yasukawa K, et al.** 1994. Azaphilones inhibit tumor promotion by 12-O-tetradecanoylphorbol-13-acetate in two-stage carcinogenesis in mice. Oncology **51**:108–112.
74. **Yu JH, Keller N.** 2005. Regulation of secondary metabolism in filamentous fungi. Annu. Rev. Phytopathol. **43**:437–458.
75. **Zähner H, Drautz H, Weber W.** 1982. Novel approaches to metabolite screening, p 51–70. *In* Bu'lock JD, Nisbet LJ, Winstanley DJ (ed), Bioactive microbial products: search and discovery. Academic Press, New York, NY.
76. **Zerikly M, Challis GL.** 2009. Strategies for the discovery of new natural products by genome mining. Chembiochem **10**:625–633.
77. **Zhang H, Boghigian BA, Armando J, Pfeifer BA.** 2011. Methods and options for the heterologous production of complex natural products. Nat. Prod. Rep. **28**:125–151.